



**The effect of Nordmøre grid length and angle on codend
entry of bycatch fish species and shrimp catches**

Journal:	<i>Canadian Journal of Fisheries and Aquatic Sciences</i>
Manuscript ID	cjfas-2018-0069.R1
Manuscript Type:	Article
Date Submitted by the Author:	09-May-2018
Complete List of Authors:	Larsen, Roger; The Arctic University of Norway UIT, The Norwegian College of Fishery Science; Sistiaga, Manu; SINTEF Fisheries and Aquaculture, Fisheries Technology Herrmann, Bent; SINTEF Fisheries and Aquaculture, Fishing Gear Technology Brinkhof, Jesse ; The Arctic University of Norway, The norwegian College of Fisheries Sciences Tatone, Ivan; University of Tromsø, Norwegian College of Fisheries and Aquatic Sciences Santos, Juan; Thuenen Institute for Baltic Sea Fisheries,
Keyword:	Shrimp trawl, bycatch reduction, grid angle, grid length, size selectivity
Is the invited manuscript for consideration in a Special Issue? :	N/A

SCHOLARONE™
Manuscripts

The effect of Nordmøre grid length and angle on codend entry of bycatch fish species and shrimp catches

Roger B. Larsen^{1a*}, Manu Sistiaga^{2*}, Bent Herrmann^{1,2*}, Jesse Brinkhof^{1,2}, Ivan Tatone¹, Juan Santos³.

¹ The Arctic University of Norway, UiT, Breivika, N-9037 Tromsø, Norway

² SINTEF Ocean, Brattørkaia 17C, N-7010 Trondheim, Norway

³ Thünen Institute of Baltic Sea Fisheries, Alter Hafen Süd 2, 18069 Rostock, Germany

^a Corresponding author. Tel: +4777644536

*Equal authorship.

E-mail address: roger.larsen@uit.no

Abstract

The Nordmøre grid is regarded as an efficient bycatch reducing device and is used in various shrimp trawl fisheries globally. However, in some shrimp fisheries bycatch remains a problem that seriously impacts commercial trawl activities. This study tested and compared the performance of two versions of the Nordmøre grid in the Northeast Arctic Deepwater Shrimp (*Pandalus borealis*) fishery; a standard version with an operating angle of ca. 45° and a longer version of the grid (40% longer) with an operating angle of ca. 30°. The grid passage probability for the bycatch of juvenile Cod, Haddock, American Plaice and Redfish increased significantly for certain size ranges of fish when using the longer grid. The longer grid also resulted in a significant increase in grid passage probability for large shrimp. Previous studies have reported that a reduced operating angle can lead to a lower grid passage probability for bycatch fish species and shrimp, however the results of the current study demonstrate that a longer Nordmøre grid more than compensates for the reduced operational angle.

Keywords: Shrimp trawl, bycatch reduction, grid angle, grid length, size selectivity

1. Introduction

26 Bycatch of juvenile fish in shrimp trawl fisheries has been investigated globally and has been
27 widely reported in the literature (e.g. Broadhurst 2000; Eayrs 2007). The introduction of the
28 Nordmøre grid in 1991 (Isaksen et al. 1992) marked a significant breakthrough in reducing
29 the incidental capture of juvenile fish in shrimp fisheries. The device was not only adopted in
30 Scandinavia and the Northeast Atlantic fisheries, where it was originally introduced, but also
31 in countries such as Canada, Iceland, Australia and the USA (Hickey et al. 1993;
32 Thorsteinsson 1995; Broadhurst and Kennelly 1996; He and Balzano 2007). While the
33 introduction of the Nordmøre grid and other types of sorting grids have considerably reduced
34 juvenile fish bycatch in shrimp fisheries (He and Balzano 2012), bycatch remains a problem
35 that can impact fishery activity. In Norway, if numbers of juvenile fish bycatch exceeds a
36 given limit, the fishing grounds are closed, which can have serious consequences for
37 fishermen with regard to the areas they can operate in and sailing distances to fishing grounds
38 (Gullestad et al. 2015). In addition, high numbers of juvenile fish in the catch can result in
39 additional sorting work onboard and a reduction in shrimp quality, due to longer catch
40 manipulation time. High levels of juvenile mortality can also have serious consequences for
41 fish stocks, in addition to the environmental and ethical implications of bycatch.

42 In the Northeast Arctic fishery for Deepwater Shrimp (*Pandalus borealis*), a Nordmøre grid
43 with a maximum bar spacing of 19 mm and a diamond mesh codend with a minimum mesh
44 size of 35 mm is compulsory selectivity gear (Larsen et al. 2017). The working principle of
45 the Nordmøre grid was first described by Isaksen et al. (1992). In this system all catch is
46 directed towards the grid by a guiding funnel and sorted by a sorting grid installed at an angle
47 of ca. 45°. The sorting grid covers the whole cross-section area of the grid section and the
48 distance between the guiding funnel (or guiding panel) and the grid is at least 50 cm. The
49 shrimp and bycatch that pass between the bars of the grid continue to move towards the

50 codend, while the fish and shrimp that are not able to pass through the grid are diverted
51 towards the bycatch outlet on the upper panel and subsequently escape (Fig. 1).

52 Fig 1.

53 There have been numerous attempts to improve the release efficiency of juvenile fish with the
54 Nordmøre grid by changing its design or by adding additional devices (e.g. Fonseca et al.
55 2005; He and Balzano 2011). One of the most obvious ways of modifying the selective
56 properties of the grid without making any design changes to the grid itself, is the manipulation
57 of its operating angle. Broadhurst et al. (2004) compared a conventional Nordmøre grid to a
58 longer grid and found no significant differences in neither prawns nor fish bycatch in an
59 Australian penaeid trawl fishery. A study by Grimaldo (2006) in the Norwegian shrimp-trawl
60 fishery showed that reducing the grid angle increases the percentage of bycatch escaping
61 through the bycatch outlet. However, the study also showed that reducing the angle resulted in
62 a higher loss of the target species (shrimp) through the bycatch outlet. Currently, Norwegian
63 inshore and coastal shrimp trawlers fish with a small grid (1.3–1.5 m length) at an operating
64 angle of ca. 45°. The majority of offshore shrimp trawlers use larger grids (2.0–2.5 m) at
65 similar grid angles, but some fishermen prefer using grid angles of 35°–40°. Decreasing the
66 operational angle of the sorting grid results in a reduced distance to the outlet, which may be
67 the reason for the greater loss of shrimp. However, a lower grid angle may also enable fish to
68 avoid the grid and increase the number directed towards the outlet. In the current study
69 experimental fishing was carried out using a longer version of the Nordmøre grid. This longer
70 version facilitated a reduced grid angle without having to reduce the vertical distance in the
71 grid section. It was hypothesized that as the vertical distance in the section was kept equal,
72 any potential increase in shrimp loss would be minimized, and that due to the reduced angle,
73 fish could escape more easily through the bycatch outlet (Grimaldo 2006), without contacting
74 the grid. In this manner, the lower grid angle would minimize the risk of fish passing through

the grid and entering the codend. Furthermore, it is possible that this grid design could result in improved shrimp catches, due to the increased area and time for shrimp to contact the grid (Sistiaga et al. 2010).

The following research questions were examined in this study:

- Does a longer Nordmøre grid with a reduced angle facilitate increased escape of juvenile fish through the outlet?
- Is the effect of using a longer grid similar for all fish bycatch species?
- Does a longer Nordmøre grid prevent the loss of commercial sizes of Deepwater shrimp?

2. Material and methods

2.1 Experimental design

Fishing trials were carried out onboard the Research Vessel (R/V) "Helmer Hanssen" (63.8 m total length and 4,080 HP) between the 16th and 28th of February 2017, in the northern part of the Barents Sea (i.e. east of Hopen Island, N 76°00', E 32°00'). Two identical Campelen 1800# trawls built entirely of 40–80 mm diamond mesh (2 mm polyethylene [PE] twine) were alternated during trials. The ground gear of each of the trawls was 19.2 m long and was built of three sections with 46 cm rubber discs. Thyborøn T2 trawl doors (6.5 m² and 2,200 kg) were used. Independent of the towing depth, the door distance was kept constant at 48–52 m at a towing speed of 1.5–1.6 m s⁻¹. The door distance was kept constant by means of a 20 m long restrictor rope that was linked between the warps 80 m in front of the doors to minimize geometrical changes of the ground gear and trawl opening. The geometry of the trawl was monitored with Scanmar instruments (<http://www.scanmar.no>) via a set of door sensors and a height sensor. The bridles between the doors and the trawl were 40 m long.

Each trawl was equipped with a four-panel grid section as illustrated in Fig. 2. The grid section and transition sections were built from 50 mm mesh (2 mm, polyamide [PA]) netting. The only differences between the two grid sections were that the Nordmøre grids were of different sizes and installed at different operating angles. The first grid, which is the standard grid used by the Norwegian coastal fleet targeting shrimp, was 1500 mm long and 750 mm wide (short grid). This grid was mounted so that it would be maintained at an angle of $45.0 \pm 2.5^\circ$ while fishing. The second grid was 2100 mm long and 750 mm wide (long grid) and was mounted so that it would be maintained at an angle of $30.0 \pm 2.5^\circ$ while fishing. Both grids were made of aluminum and had almost identical bar spacing of 18.8 ± 0.4 mm (mean \pm SD) and 18.9 ± 1.2 mm for the short grid and long grid, respectively. The bar spacing was measured with a caliper following the guidelines described in Wileman et al. (1996). The escape opening was cut out of the top panel of the grid section and formed a 35-mesh long and 70-mesh wide triangle, i.e. 0.75 m wide and ca. 1.60 m long.

Fig 2.

The fish and shrimp exiting through the escape outlet in each of the sections were collected by similar covers made of 48 mm (2.1 mm PE twine) and 35 mm (1.8 mm PA twine) diamond meshes (Fig. 3). Both covers were blinded by small mesh netting (liners) with an average mesh size of 16.4 ± 0.5 mm in the short grid cover, and 16.0 ± 1.0 mm in the long grid cover. The codends attached to the grid sections in both trawls were built of ca. 35 mm meshes (2 mm PA twine) and were blinded by small mesh liner of diamond netting (18.5 ± 0.5 mm).

Fig 3.

The catch from the different compartments in the gear was kept separate at all times. The catch in each compartment was sorted by species and all fish bycatch species were measured to the nearest centimeter. No subsampling was carried out for any of the fish species, except

for American plaice in haul 12 and redfish in haul 18. Due to the high volume of shrimp, it was not possible to measure the entire catch and a subsample was randomly taken from each compartment for all hauls. Each subsample weighed ca. 1 kg, which was determined to adequately represent the size distribution of shrimp in that specific compartment. The carapace of the shrimp was measured to the nearest millimeter using a caliper.

To study shrimp and fish behavior with respect to the two grids tested, a camera system comprised of a stainless-steel frame, a GoPro Hero 4 Black Edition camera (San Mateo, California, USA) protected by a stainless-steel housing (iQsub Technologies, Czech Republic), and two red light emitting diode (LED) lamps with batteries (Brinyte®, DIV01C-V and type CREE XPE R5, Shenzhen Yeguang Technology Co., Ltd, China) was used. Red LEDs were selected as previous studies (e.g. Anthony and Hawkins 1983) have shown that red light affects fish behavior less than the more-traditionally used white lights. Recently Nguyen et al. (2017) found similar effects with red LED lamps in a study on crustaceans, i.e. snow crab (*Chionoecetes opilio*). The camera was attached to the upper panel ca. 1.7 m ahead of the grid, above the end of the guiding panel and facing the grid in all cases.

2.2 Size selection models

Larsen et al. (2017) used the following model to describe the size dependent probability of a shrimp or fish passing through the Nordmøre grid and entering the codend ($p(l)$):

$$p(l, C_{grid}, \mathbf{v}) = C_{grid} \times (1.0 - rc(l, \mathbf{v}))(1)$$

Since the experimental design of the current study is similar to that in Larsen et al. (2017), we will use the same structure for model (1) to describe the size dependent probability of fish bycatch species and shrimp passing through the Nordmøre grid. In (1) l represents the length of the fish or carapace length of shrimp. The probability of contacting the grid is modeled by the length independent parameter C_{grid} which has a value ranging from 0.0 to 1.0. An

146 estimated C_{grid} value of 1.0 for a species means that every individual of that species contacts
147 the grid in a way that gives them a length dependent chance of passing through the grid. In the
148 case of an individual fish or shrimp not contacting the grid, or being poorly oriented during
149 contact, it will be reflected in the C_{grid} value. For fish or shrimp contacting the grid, the size
150 selectivity function $rc(l, \mathbf{v})$ models the length dependent probability of passing through the
151 Nordmøre grid conditioned contact. The vector \mathbf{v} represents the parameters of this selectivity
152 model. Larsen et al. (2017) applied the standard logit size selection model (Wileman et al.
153 1996) for $rc(l, \mathbf{v})$. In this case \mathbf{v} contains two parameters: $L50_{grid}$ which denotes the length of
154 the species with a 50% probability of being prevented from passing through the grid, and
155 SR_{grid} which describes the difference in length between individuals with a 75% and 25%
156 probability of being prevented from passing through the grid. Further details on model (1) and
157 the parameters of this model are provided in Larsen et al. (2017). In addition to the *Logit*
158 model, three other size selection models *Probit*, *Gompertz* and *Richard* (Wileman et al. 1996)
159 were applied as candidates for $rc(l, \mathbf{v})$ because this collection of S-shaped size selection
160 models has been found to be well-suited for modelling basic size selection processes in trawls
161 in several studies (Wileman et al. 1996; Brčić et al. 2016; Santos et al. 2016a; Sistiaga et al.
162 2016; Stepputtis et al. 2016). For the *Probit* and *Gompertz* models the parameters are the
163 same as the Logit model, while the *Richard* model requires an additional parameter $1/\delta$ that
164 models asymmetry (Appendix; Wileman et al. 1996). In addition, to allow the contact
165 parameter C_{grid} take a value below 1.0, the case where this is fixed to 1.0 was also considered,
166 meaning that it is assumed all fish or shrimp will make contact with the Nordmøre grid.
167 Therefore, eight different models were considered for $p(l, C_{grid}, \mathbf{v})$.

168 As species differ in morphology and behavior, values of the parameters C_{grid} and \mathbf{v} will be
169 species specific, for the same selective system. Therefore, model (1) needs to be applied
170 separately for Deepwater shrimp and individual bycatch species, in addition to being applied

separately for the long and short Nordmøre grid. To determine how each of the Nordmøre grid configurations performed on average, analysis was carried out for data summed over all hauls. The analysis was conducted separately for each Nordmøre grid configuration based on the data from the hauls with the specific configuration and separately for each species. Thus, function (2) was minimized, which is equivalent to maximizing the likelihood for the observed data in form of the length dependent number of individuals measured as retained in the codend (nC_l) versus collected in the Nordmøre grid cover (nG_l).

$$-\sum_{j=1}^m \sum_l \left\{ \frac{nC_{jl}}{qC_j} \times \ln \left(p(l, C_{grid}, \mathbf{v}) \right) + \frac{nG_{jl}}{qG_j} \times \ln \left(1.0 - p(l, C_{grid}, \mathbf{v}) \right) \right\} \quad (2)$$

where qC_j and qG_j represent the sampling factors for the fraction of individuals measured in the blinded codend and grid cover for each haul j . The sampling factors can take a value ranging from 0.0 to 1.0 (1.0 if all individuals are length measured). The outer summation in (2) is for the hauls conducted with the specific Nordmøre grid configuration and the inner summation is for length classes in the data (Larsen et al. 2017).

Each of the eight candidate models for $p(l, C_{grid}, \mathbf{v})$ were fitted to the experimental data using expression (2). The model resulting in the lowest Akaike information criterion (AIC) value (Akaike 1974) was selected separately for each species and each grid to model the grid passage probability.

The ability of the selected model for $p(l, C_{grid}, \mathbf{v})$ to describe the data sufficiently, was based on calculating the corresponding p-value. In the case of poor fit statistics (p-value < 0.05), the residuals were inspected to determine whether the poor result was due to structural problems when modelling the experimental data (model [1]), or if it was due to over-dispersion in the data (Wileman et al. 1996).

Efron 95% percentile confidence bands (Efron 1982) for the grid passage probability curve (model (1)), and the parameters in it (C_{grid}, \mathbf{v}), were obtained using a double bootstrap method

implemented in the software tool SELNET (Herrmann et al. 2012) which was applied for the analysis. For each species and grid configuration analyzed, 1000 bootstrap repetitions were conducted to estimate the 95% confidence limits (Efron percentile) (further details are given in Larsen et al. 2017).

To infer the effect of changing from a short to a long Nordmøre grid on grid passage probability, the change in the length dependent grid passage probability $\Delta p(l)$ was estimated:

$$\Delta p(l) = p_{long}(l) - p_{short}(l) \quad (3)$$

where $p_{short}(l)$ is the grid passage probability obtained for the short Nordmøre grid and $p_{long}(l)$ is the grid passage probability obtained for the long Nordmøre grid. Efron 95 % percentile confidence limits for $\Delta p(l)$ were obtained based on the two bootstrap populations of results (1000 bootstrap repetitions in each) for both $p_{short}(l)$ and $p_{long}(l)$. As they are obtained independently, a new bootstrap population of results was created for $\Delta p(l)$ by:

$$\Delta p(l)_i = p_{long}(l)_i - p_{short}(l)_i \quad i \in [1 \dots 1000] \quad (4)$$

where i denotes the bootstrap repetition index. As the bootstrap resampling was random and independent for the two groups of results, it is valid to generate the bootstrap population of results for the difference based on (4) using the two independently generated bootstrap files (Moore et al. 2003). Based on the bootstrap population, Efron 95 % percentile confidence limits can be obtained for $\Delta p(l)$ as described above.

2.3 Catching efficiency indicators

The former section described how the performance of the two grids is quantified in terms of the length-dependent grid passage probability. The benefit of this approach is that ideally it provides an estimate that is independent on the specific population structures fished on, which allows extrapolation of the results to other fishing scenarios. However, the approach also has a limitation as it does not provide a direct quantification of the consequences of using the

grids in the specific fishing situation. This would require a measure that is dependent on the population structures fished on. Therefore, to supplement the evaluation of the grids based on length-dependent grid passage probability, we also estimated the catch efficiency indicator nP_+ , directly from the catching data:

$$nP_+ = 100 \times \frac{\sum_j \sum_{l>MLS} \left\{ \frac{nC_{jl}}{qC_j} \right\}}{\sum_j \sum_{l>MLS} \left\{ \frac{nC_{jl}}{qC_j} + \frac{nG_{jl}}{qG_j} \right\}} \quad (5)$$

Where the outer summation of j is over hauls with the specific grid, and l is over length classes. nP_+ quantifies the grid passage efficiency of the population encountered during the trials for the sizes above MLS (Minimum Landing Size) of the species investigated. Equation (5) was applied separately for each species and each grid. For deep-water shrimp we used a MLS at 15 mm carapace length because this is the minimum size allowed. For each of the bycatch species we used total length above zero cm as all sizes are unintended catch. For a grid to perform well in the specific fishery, accounting explicitly for the population structures fished on, nP_+ should be close to 100% for target species and as low as possible for unintended species (close to 0 %). This concept of supplementing the size selectivity curve based evaluation with catch efficiency indicators like nP_+ , was first described and used by Wienbeck et al. (2014) and later used in other studies (Sala et al. 2015; Brčić et al. 2015; Santos et al. 2016b; Lövgren et al. 2016).

We used the bootstrapping methods and software tool described in the previous section to estimate the Efron 95% percentile confidence bands for nP_+ . The confidence bands were estimated for each species and for respectively the short and long grid as well as for their difference in value ($\Delta nP_+ = nP_{+long} - nP_{+short}$).

3 Results

A total of 20 hauls were carried out during the experimental period, 10 with the short grid and 10 with the long grid. Of all the relevant bycatch species in the Northeast Atlantic Deepwater shrimp fishery, cod (*Gadus morhua*), haddock (*Melanogrammus aeglefinnus*), American plaice (*Hippoglossoides platessoides*) and redfish (*Sebastes* spp.) were captured in sufficient numbers to be included in the analyses. Length measurements were taken for 5386 shrimp, 6536 redfish, 10175 American plaice, 2057 cod and 6278 haddock from the grid cover (*ng*) and codend (*nc*). An overview of the hauls and the number of shrimp and bycatch fish species measured from each of the compartments is given in Table 1.

Table 1

In some cases, the deep-water shrimp catches were subsampled even if the catch in the specific compartment was small (less than 1 kg) because some of the shrimps were damaged and did not allow a reliable measurement of their carapace length (Table 1).

The *Gompertz* model with fixed C_{grid} best described the shrimp data for both the long and short grids (Table 2). For redfish, the *Probit* model with estimated C_{grid} best described data collected with the short grid, while the *Logit* model with estimated C_{grid} provided lowest AIC value for the long grid. For American plaice, the *Gompertz* model with estimated C_{grid} resulted in the lowest AIC value for both the short and the long grid data. Regarding cod, the *Probit* model with estimated C_{grid} and the *Richard* model with fixed C_{grid} resulted in the models with the lowest AIC value for the short grid and long grid, respectively. For haddock, the *Richard* model with fixed C_{grid} was also resulted in the lowest AIC for the long grid. However, for the short grid the model with the best fit was the *Richard* model with estimated C_{grid} . Note that for each case analyzed, there were alternative models with AIC values within +2.0, which means that the support for these other models was also strong. However, based on an explorative analysis (not presented here), we could see that these alternative models

always led to a nearly identical estimate of grid passage probability as the model with lowest AIC. This was observed at least for the length range where the estimation was supported by the experimental data. Therefore, as long as we avoid extrapolations when making conclusions, we are confident in modelling the grid passage probability alone based on the models with lowest AIC values.

Table 2.

The fit statistics show that the models chosen described the data well in most cases (Table 3). The p-value was >0.05 for all bycatch fish species, which means that the discrepancy between the data and the model could be due to coincidence. This is corroborated by comparing the deviance and degrees of freedom, which were of the same magnitude in all cases. For the shrimp, the p-value was <0.05 for both the short and long grids. However, this low p-value is probably a consequence of subsampling the shrimp catch, as the model represented the length dependent trend in the data well (Fig. 4). Further inspection of deviance residuals showed only few values outside the ± 2.0 limit, and these showed no clear pattern (Appendix).

The selectivity parameters obtained from the models are presented in Table 3. The average $L50_{grid}$ and SR_{grid} values obtained for shrimp are far above any biological size range for shrimp, and should therefore only be seen as parameter values that allow the model to describe the grid passage probability for the sizes of shrimp available.

Table 3.

It can be seen from Figure 4 that there is a difference between the grid passage probability with the short grid and the long grid for shrimp. The grid passage probability is higher with the long grid for all sizes of shrimp. Figure 4a and 4b show the size distribution and the passage probability for shrimp with the short (a) and long (b) grid. The difference between the grids increases with increasing shrimp size, and is significantly higher than 0.0 for shrimp

with a carapace length greater than 20 mm (Fig. 4c). Therefore, the results demonstrate that the long grid produces a higher grid passage probability for the largest shrimp. Significance is obtained although all three plots in Figure 4 show an increase in confidence bands with increase in shrimp size. This increase reflects the relative low occurrence for bigger shrimp (carapace length > 25 mm) in the catch data.

Fig 4.

For the smallest sizes of all four bycatch species, the estimated grid passage probability was significantly higher for the long grid compared with the short grid. Further, the grid passage probability significantly was for no length classes higher for the short grid. Figure 5 shows the size distribution and the passage probability for bycatch species of fish with the short (a;d;g;j) and long (b;e;h;k) grid. Grid passage probability was significantly higher for the long grid for redfish between 5 and 13 cm (Fig. 5c) and cod between 5 and 15 cm (Fig. 5f). For haddock, the delta plot shows that the grid passage probability for the long grid is on average always higher for the long grid and this difference is significant for fish 10–16 cm and 19–25 cm (Fig. 5i). American plaice between 5 and 15 cm were also found to have a significantly higher grid passage probability (Fig. 5l).

Fig 5.

In general, the results from the data analysis show that using a longer grid at a lower angle significantly increases the grid passage probability for shrimp, in particular large shrimp. Therefore, it is beneficial to use a long grid with a lower operating angle to promote the catch efficiency of the target species. However, the long grid also results in a higher grid passage probability for all bycatch species, meaning that using a longer grid at a lower angle does not promote juvenile bycatch avoidance.

The evaluation based on the nP_+ (catch efficiency indicator) values confirmed that for the specific fishery situation in the trials, the long grid would be more efficient at catching the targeted sizes of deep-water shrimp (Table 4). Specifically, 97% and 99% of the shrimp with carapace length above 15 mm passed through respectively the short and long grid. This increase by 2% for the long grid was found to be statistically significant as ΔnP_+ was significant above 0.0. For the bycatch species cod and haddock and the long grid, the results showed a significant increase in catch efficiency with estimated ΔnP_+ values of respectively 10.5 and 18%. For redfish and American plaice, the results were non-significant, which could potentially be due to variations in the population structures entering the gear between hauls, which contrary to the evaluation based on length-dependent grid passage probability, affects the evaluation based on ΔnP_+ values.

Table 4

The underwater recordings showed that the short grid with the higher angle got blocked by fish entering the section more easily than the longer grid with the lower angle. Fish are forced towards the lower grid-face due to the water flow, and the steep angle of the grid makes it difficult for fish to slide towards the bycatch outlet on top. American plaice could at some instances also cover considerable parts of the surface of the long grid. The two images shown in Fig. 6 were taken approximately 30 min after fishing had started, and show redfish covering a large area of both sides of the short grid (Fig. 6a), while there are less fish present on the long grid (Fig. 6b). The main consequence of this is that the difference in effective selective surface between the two grids, which is already ca. 40% bigger for the long grid, becomes even bigger and can have direct consequences for the selective performance of the different grids.

Fig 6.

The recordings also showed that due to the guiding funnel, both shrimp and fish entered the grid area in the section close to the lower panel. In both grid sections, most shrimp and fish made physical contact with the lowest part of the grid, and slid along the grid for a few seconds. In some cases, the fish and/or shrimp orientated themselves correctly and were subjected to the selective properties of the grid (either passed through or not, depending on their body shape). In other cases, they just slid all the way along the grid (e.g. sideways) or swam upwards towards the bycatch outlet (this behaviour was most frequently observed for small haddock). A typical example of what was observed in the recordings is illustrated in Fig. 7. As a fish enters the grid area through the guiding funnel it makes physical contact with the lowest part of the grid (Fig. 7a). The fish then moves along the entire grid face (Fig. 7b–d) until it finally orientates itself correctly towards the grid and passes through it (Fig. 7e–f). In the long grid there is an increased likelihood that an individual fish or shrimp will be able to orientate itself correctly towards the grid, due to the larger sorting area in comparison to the short grid. As presented in the introduction, one could hypothesize that due to the lower angle more shrimp and fish would escape through the bycatch outlet without contacting the grid at all when using the longer grid, but this was not supported by the underwater recordings or the trawl data collected during this study.

Fig 7.

4 Discussion

The aim of this study was to test whether a longer version of the Nordmøre grid with an increased selective surface and lower operating angle could improve the selective properties of the standard Nordmøre grid used by the Norwegian coastal shrimp vessels. It was expected that the longer grid with a lower grid angle would enable a larger fraction of juvenile fish to avoid contact with the grid (lower C_{grid}), leading to a lower grid passage probability. However, the results obtained in this study showed the opposite effect, as using the longer

grid led to significant increase in the grid passage probability for juvenile fish. This unexpected result is likely due to the fact that small fish are unable to avoid physical contact with the grid, and so the fish "slide" over a longer area of the grid than would be the case with the shorter grid. This results in a higher probability of the fish being orientated in a way that facilitates grid passage, ultimately producing a higher grid passage probability for the long grid. A higher grid passage probability was also found for Deepwater shrimp when using the long grid. The values for the catch efficiency indicator nP_+ , which account for the specific population fished on during the trials, showed a significant increase for the long grid. Specifically, the results showed that catch efficiency for the targeted sizes of deep-water shrimp would increase by 2%. However, for two of the bycatch species investigated the use of the long grid would also lead to an increase in entry to the codend, which would not be beneficial as it would lead to an increase in unintended fish mortality and in catch sorting work.

In this study, the angle of the long grid was reduced to 30° so that the long grid would cover the same vertical area as the short grid, and could be fitted to the same netting section size, i.e. with equal vertical height in the two grid sections. The literature on the effect of grid angle change and changes in grid dimensions is limited, but Grimaldo (2006) studied the effect of decreasing and increasing the angle of a cosmos grid on an offshore commercial vessel in the Barents Sea. The results showed that when the grid was installed at a lower angle (33° as opposed to 39°), there was an increase in escaping shrimp (i.e. loss of the target species) and the amount of fish released through the escape outlet of 3.4% and 9.1%, respectively. These results agreed with the expectation that lowering the grid angle reduces the vertical projected area of the grid, allowing more shrimp and fish bycatch to escape through the bycatch outlet without contacting the grid at all. In the present study, the long grid had a lower angle than the short grid, but unlike in Grimaldo (2006), the vertical area of both grids was identical. This

386 meant that the results obtained in the current study regarding grid angle differed from those
387 obtained by Grimaldo (2006), with a reduced grid angle increasing the amount shrimp and
388 bycatch fish that contacted the grid and passed through it. Grid passage probability increased
389 significantly for shrimp and four bycatch fish species, when a longer grid installed at a lower
390 angle was used. This increase was length dependent and followed a similar pattern for all four
391 bycatch fish species studied, however the difference diminished with fish size.

392 To be able to maintain the identical projected vertical area of the grid between the short and
393 the long grid, the operational angle of the longer grid needs to be reduced, which confounds
394 the variables "grid angle" and "grid length". This means that in the current study it is not
395 possible to discern to what extent each of these two variables contributes to the results
396 obtained.

397 Larsen et al. (2017) showed that a shorter guiding panel with a longer distance to the grid
398 surface increased the escape of juvenile haddock. However, 80% to 100% of four bycatch
399 species up to a species-specific size passed through the grid and were retained by the gear
400 irrespective the length of the guiding panel, i.e. 50 cm or 100 cm distance between the guiding
401 panel and the grid surface. Broadhurst et al. 2004 discussed that their finding of no difference
402 in bycatch reduction between the standard Nordmøre grid (600 mm long) and two longer (900
403 mm and 1200 mm long) Nordmøre grids installed at an operating angle of 28° could be a
404 result of guiding panel design. In their experiment they used guiding panels that extended to
405 the surface of the grid and the panel was weighted with chain links in the aft part, thus sorting
406 all specimen immediately irrespective the grid length or angle.

407 According to Grimaldo (2006) a lower grid angle should contribute to a lowered grid passage
408 probability, however, the results obtained in the current study prove that despite the reduced
409 operating angle, longer grids can significantly increase the grid passage probability for shrimp
410 and juvenile fish. Thus, it can be concluded that although previous studies have shown that

reducing the grid angle has the potential to increase the release of juvenile fish, increasing grid length more than compensates for reducing the angle and significantly increases grid passage probability of bycatch fish species through the grid. Regarding shrimp, the result was similar to that obtained for fish. The increase in grid length compensates for lowering the operational angle, which according to earlier studies (e.g. Larsen 1996; Grimaldo 2006) contributes to a lower grid passage probability and higher shrimp loss by weight. As for fish, the difference in passage probability for shrimp was also found to be length dependent. For fish, the largest differences between grids exhibited for the smallest sizes, while the highest difference between grids exhibited for the largest shrimp.

The Atlantic shrimp trawl fisheries in USA are today performed with a double sorting grid system with the aim to reduce the amount of juvenile fish and small shrimp (ASMFC 2017). A similar double grid system was tested in the Norwegian shrimp trawl fisheries in the end of the 1990'ties. The extra 10 mm grid in front of the 19 mm Nordmøre grid was not accepted by the industry because they claimed it stopped functioning due to clogging of the grid face shortly after tow start (Larsen pers. comm.). The Norwegian shrimp fishers have experience with longer Nordmøre grids and they find them more convenient to operate than a double grid system.

Observations from the underwater recordings in our trials corroborated the results obtained from the data analysis. Despite its lower angle, fish and shrimp were observed to physically contact the long grid at the outlet of the guiding funnel, i.e. at the lowest part of the long grid. In addition, in most cases fish and shrimp remained close to, or in physical contact with, the grid along its full extent. This explains the results obtained from the data analysis as the larger sorting area of the long grid gives fish and shrimp more time and a larger area to orientate themselves properly towards the grid and pass through it. Furthermore, the longer grid had a lower probability of being blocked by fish, further increasing the area difference between the

two grids. This difference between the grids and the probability of fish and shrimp to orientating themselves correctly towards the grid was also observed in the results obtained for the parameter C_{grid} , which was on average as high or higher for the long grid with the lower angle in every case. Plastic bags and similar manmade garbage, seaweed, stones, etc. can also block areas of the sorting grid. When C_{grid} is reduced, shrimp loss increases. The reduced angle of the sorting grid enables faster and easier removal of debris and garbage, and so has practical benefits.

The results obtained in this study also show that the size difference between the grids used by the Norwegian inshore, coastal and offshore shrimp vessels probably explains why the two fisheries use different operating grid angles. If the offshore vessels were using the same angle as the coastal vessels, the grid passage probability for bycatch species would most likely be too high due to the increased grid length.

Acknowledgements

We thank the crew of RV “Helmer Hanssen” and assistants Helene Gjesteland, Hanna Danielsen, Nadine Jacques, John T. Eilertsen, Ilmar Brinkhof and Hermann Pettersen for valuable assistance on board. We appreciate the efforts of the editor, associate editor and the two anonymous reviewers, which we feel improved our manuscript significantly. We are also grateful to the Arctic University of Norway UIT in Tromsø and the Norwegian Seafood Research Fund for funding the experiments carried out in this study.

References

- Akaike, H. 1974. A new look at the statistical model identification. IEEE Trans. Autom. Control 19 (6), 716–723.
- Anthony, P. D. and Hawkins, A. D. 1983. Spectral sensitivity of the cod, *Gadus morhua* L. Mar. Behav. Physiol. 10, 145–165.

- 460 Atlantic States Marine Fisheries Commission (ASMFC) 2017. Amendment 3 to the Interstate
461 Fishery Management Plan for Northern Shrimp, October 2017, 1-102.
- 462 Brčić, J., Herrmann, B. and Sala, A. 2015. Selective characteristics of a shark-excluding grid
463 device in a Mediterranean trawl. *Fish. Res.* 172, 352–360.
- 464 Brčić, J., Herrmann, B. and Sala, A. 2016. Can a square-mesh panel inserted in front of the
465 codend improve the exploitation pattern in Mediterranean bottom trawl fisheries? *Fish. Res.*
466 183, 13–18.
- 467 Broadhurst, M. K., Young, D. J. and Damiano, C. 2004. Effects of Nordmøre-grid angles,
468 profiles and other industry-developed modifications on catches in an Australian penaeid-trawl
469 fishery. *Ciencias Marinas* 30 (1b), 155–168.
- 470 Broadhurst, M.K. 2000. Modifications to reduce bycatch in prawn trawls: a review and
471 framework for development. *Rev. Fish Biol. Fish.* 10, 27–60.
- 472 Broadhurst, M.K. and Kennelly, S.J. 1996. Rigid and flexible separator
473 panels in trawls that reduce the by-catch of small fish in the Clarence River prawn-trawl
474 fishery, Australia. *Mar. Freshwater Res.*, Vol. 47: 991–998.
- 475 Eayrs, S. 2007. A Guide to Bycatch Reduction in Tropical Shrimp-Trawl Fisheries, Revised
476 Edition. Food and Agriculture Organization of the United Nations, Rome. ISBN: 978-92-5-
477 105674-5.
- 478 Efron, B. 1982. The jackknife, the bootstrap and other resampling plans. *SIAM Monograph*
479 No 38, CBMS-NSF.
- 480 Fonseca, P., Campos, A., Larsen, R.B., Borges, T.C. and Erzini, K. 2005. Using a modified
481 Nordmøre grid for by-catch reduction in the Portuguese crustacean-trawl fishery. *Fish. Res.*
482 71, 223–239.

- 483 Grimaldo, E. 2006. The effects of grid angle on a modified Nordmøre-grid in the Nordic
484 shrimp fishery. *Fish. Res.* 77, 53–59.
- 485 Gullestad, P., Blom G., Bakke G. and Bogstad, B. 2015. The “Discard Ban Package”:
486 Experiences in efforts to improve the exploitation patters in Norwegian fisheries. *Marine*
487 *Policy* 54 (2015) 1–9. <https://doi.org/10.1016/j.marpol.2014.09.025>.
- 488 He, P. and Balzano, V. 2012. The effect of grid spacing on size selectivity of shrimps in a
489 pink shrimp trawl with a dual-grid size-sorting system. *Fish. Res.* 121–122, 81–87.
- 490 He, P. and Balzano, V. 2011. Rope Grid: a new grid design to further reduce finfish bycatch
491 in the Gulf of Maine pink shrimp fishery. *Fish. Res.* 111, 100–107.
- 492 He, P. and Balzano, V. 2007. Reducing small shrimp in the Gulf of Maine pink shrimp fishery
493 with a new size-sorting grid system. *ICES J. Mar. Sci.* 64, 1551–1557.
- 494 Herrmann, B., Sistiaga, M. B., Nielsen, K. N. and Larsen, R. B. 2012. Understanding the size
495 selectivity of redfish (*Sebastes* spp.) in North Atlantic trawl codends. *J.Northw.Atl.Fish.Sci.*
496 44, 1–13.
- 497 Hickey, W. M., Brothers, G. and Boulos, D.L. 1993. By-catch reduction in the northern
498 shrimp fishery. Canadian Technical Report of Fisheries and Aquatic Sciences No. 1964, vi -
499 41.
- 500 Isaksen, B., Valdemarsen, J. W., Larsen, R. B. and Karlsen, L. 1992. Reduction of fish by-
501 catch in shrimp trawl using a rigid separator grid in the aft belly. *Fish. Res.*, 13: 335–352.
- 502 Larsen, R.B. 1996. Experiments with a new, larger type of fish/shrimp separator grid with
503 comparisons to the standard Nordmøre-grid. In: ICES CM 1996/B:1, Report of the study

- 504 group on grid (grate) sorting systems in trawls, beam trawls, and seine nets, Woods Hole,
505 Massachusetts, 13–14 April, 1996, pp. 68–80.
- 506 Larsen, R.B., Herrmann, B., Sistiaga, M., Brinkhof, J. Tatone, I. and Langård, L. 2017.
507 Performance of the Nordmøre grid in shrimp trawling and potential effects of guiding funnel
508 length and light stimulation. Marine and Coastal Fisheries,
509 [dx.doi.org/10.1080/19425120.2017.1360421](https://doi.org/10.1080/19425120.2017.1360421).
- 510 Larsen, R.B. The Arctic University of Norway, UiT, Breivika, N-9037 Tromsø, Norway,
511 personal communication, 2018.
- 512 Lövgren, J., Herrmann, B. and Feekings, J. 2016. Bell-shaped size selection in a bottom trawl:
513 A case study for Nephrops directed fishery with reduced catches of cod. Fish. Res. 184, 26–
514 35.
- 515 Moore, D.S, McCabe, G.P., Duckworth, W.M. and Sclove, S.L. 2003. Practice of Business
516 Statistics using data for decisions. Published by W. H. Freeman. ISBN 10: 0716757230 /
517 ISBN 13: 9780716757238.
- 518 Nguyen, K.Q., Winger P.D., Morris, C. and Grant, S.M. 2017. Artificial lights improve the
519 catchability of snow crab (*Chionoecetes opilio*) traps. Aquaculture and Fisheries 2, 124-133.
- 520 Sala, A., Lucchetti, A., Perdichizzi, A., Herrmann and Rinelli, P. 2015. Is square-mesh better
521 selective than larger mesh? A perspective on fisheries management for Mediterranean trawl
522 fisheries. Fish. Res. 161, 182–190.
- 523 Santos, J., Herrmann, B., Otero, P., Fernandez, J. and Pérez, N. 2016a. Square mesh panels in
524 demersal trawls: Does the lateral positioning enhance fish contact probability? Aquat. Living
525 Resour. 29: 302. DOI: 10.1051/alr/2016025.

- 526 Santos, J., Herrmann, B., Mieske, B., Stepputtis, D., Krumme, U. and Nilsson, H. 2016b.
527 Reducing flatfish by-catches in roundfish fisheries. *Fish. Res.* 184, 64–73.
- 528 Sistiaga, M., Herrmann, B., Grimaldo, E. and Larsen, R.B. 2010. Assessment of dual selection
529 in grid based selectivity systems. *Fish. Res.* 105, 187–199.
- 530 Sistiaga, M., Brinkhof, J., Herrmann, B., Grimaldo, E., Langård, L. and Lilleng, D. 2016. Size
531 selective performance of two flexible sorting grid designs in the Northeast Arctic cod (*Gadus*
532 *morhua*) and haddock (*Melanogrammus aeglefinus*) fishery. *Fish. Res.* 183, 340–351.
- 533 Stepputtis, D., Santos, J., Herrmann, B. and Mieske, B. 2016. Broadening the horizon of size
534 selectivity in trawl gears. *Fisheries Research* 184, 18–25.
- 535 Thorsteinsson, G. 1995. Survival of shrimp and small fish in the inshore shrimp fishery at
536 Iceland. ICES Study Group on Unaccounted Fishing Mortality in Fisheries Aberdeen, 17–18.
537 April 1995, 13 pp.
- 538 Wienbeck, H., Herrmann, B., Feekings, J.P., Stepputtis, D. and Moderhak, W. 2014.
539 Comparative analysis of legislated and modified Baltic Sea trawl codends for simultaneously
540 improving the size selection of cod (*Gadus morhua*) and plaice (*Pleuronectes platessa*). *Fish.*
541 *Res.* 150, 28–37.
- 542 Wileman, D.A., Ferro, R.S.T., Fonteyne, R. and Millar, R.B. (Eds.) 1996. Manual of Methods
543 of Measuring the Selectivity of Towed Fishing Gears. ICES Cooperative Research Report No.
544 215, Copenhagen, 126 pp.

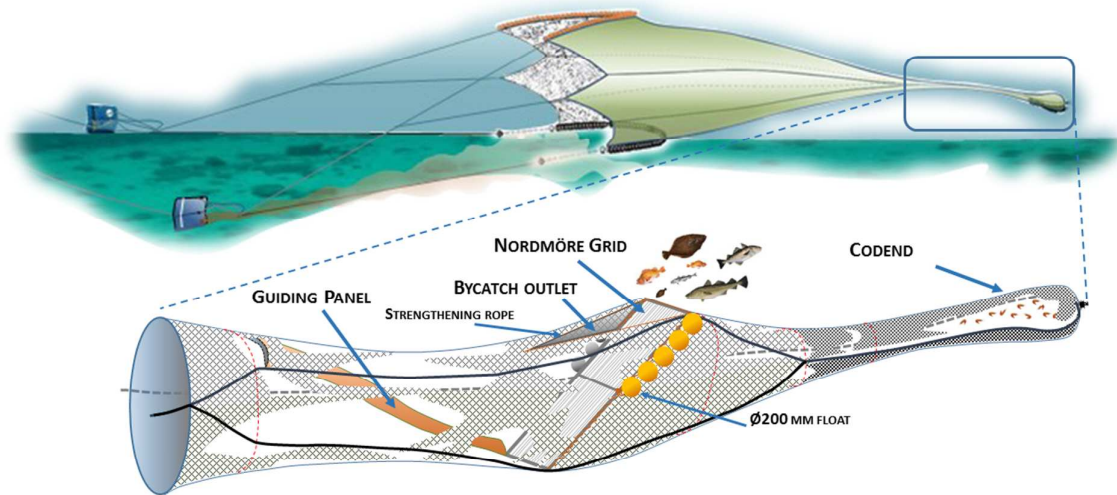


Figure 1: Illustration of the working principle of the Nordmøre grid.

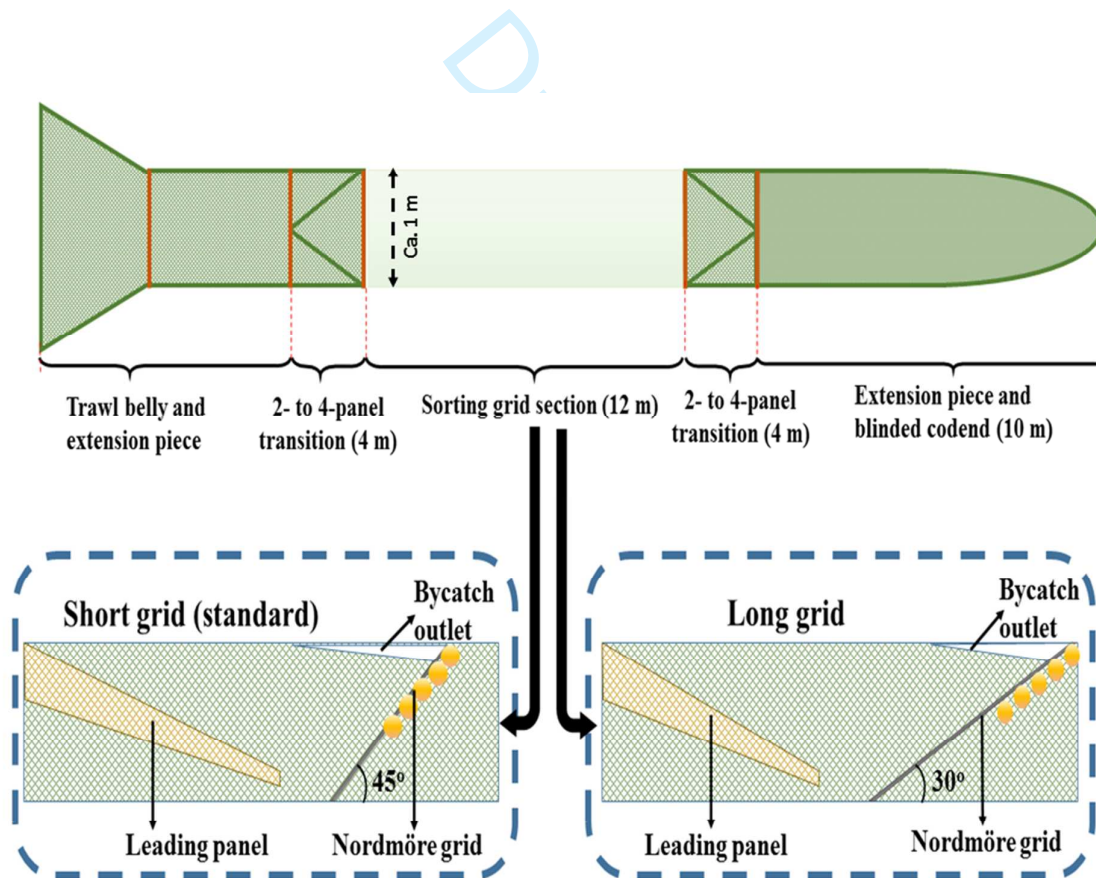


Figure 2: Side view of the aft section of the trawl and the two sorting grid designs (short grid and long grid) tested during the experiments.

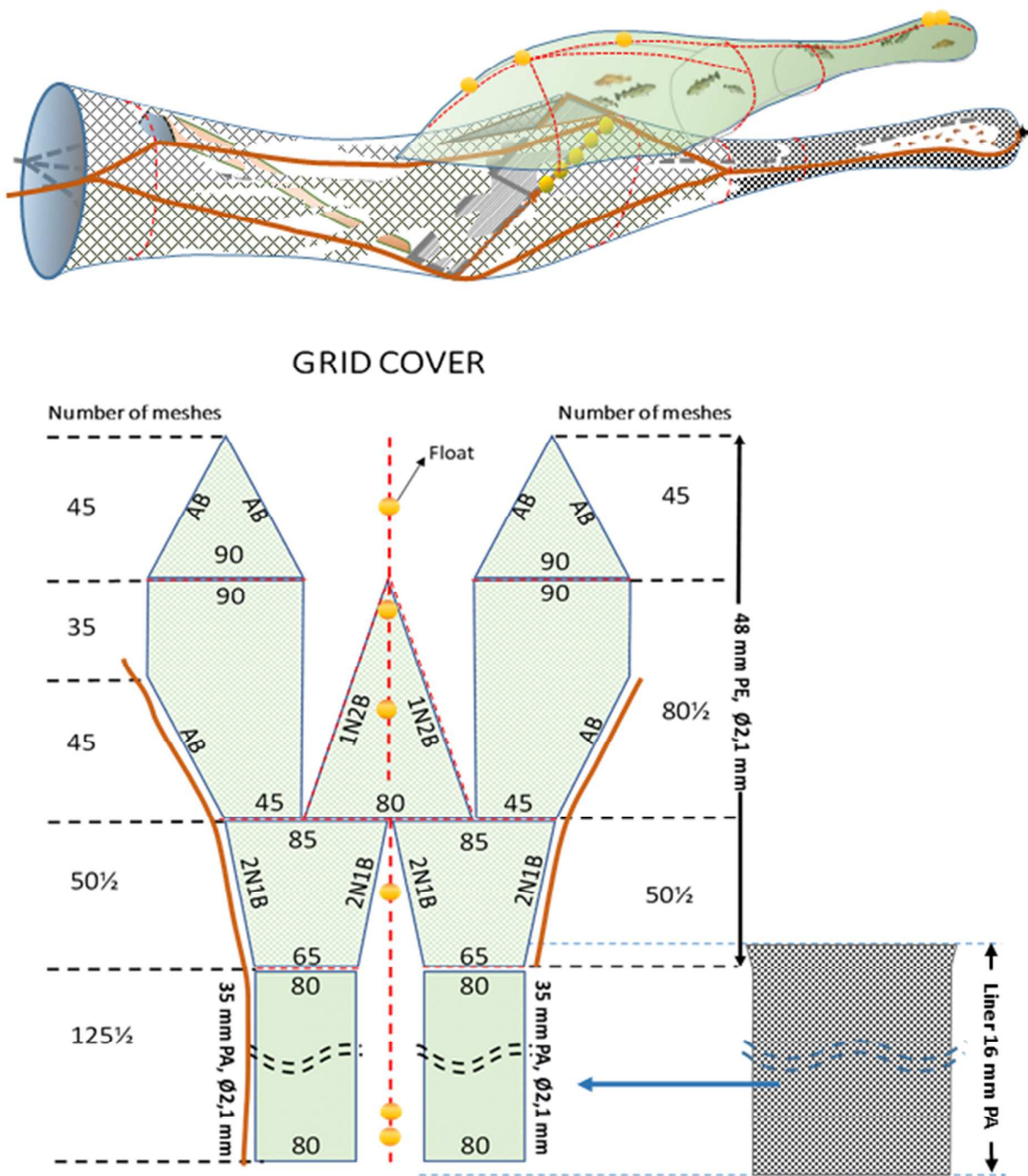


Figure 3: Technical drawing of the covers used during the experiments.

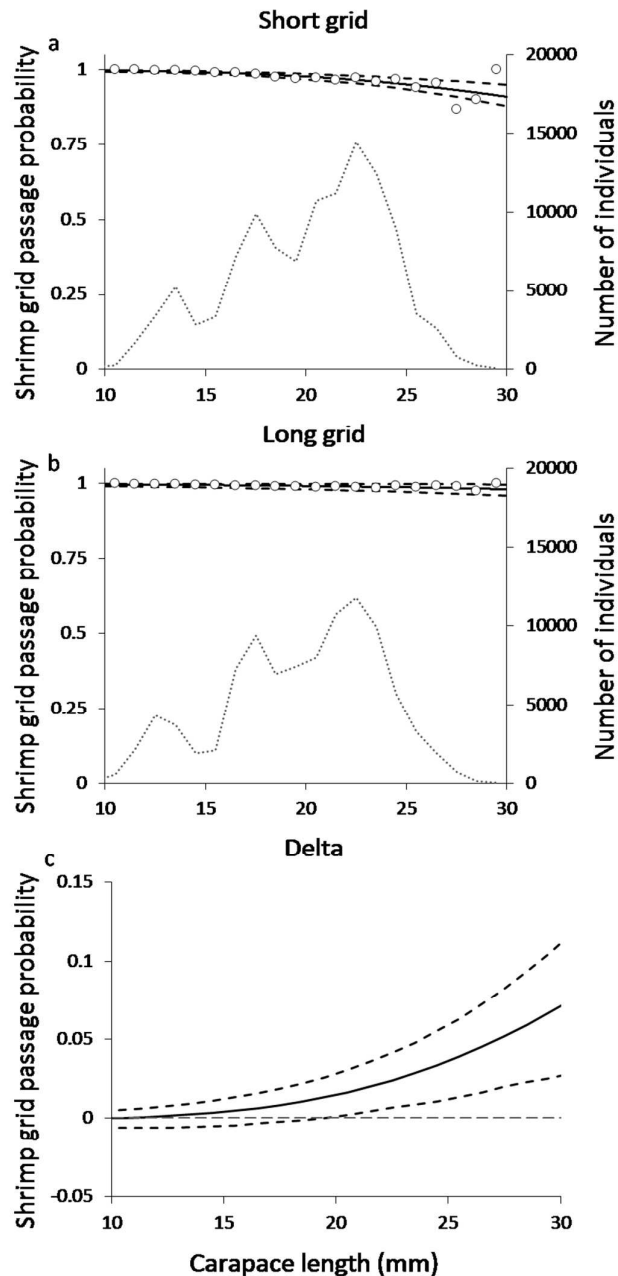


Figure 4: Size distribution and grid passage probability for shrimp with the short grid (a), long grid (b) and the difference (Delta) between both grids (c). The circles represent the experimental data collected during the cruise. The solid black line illustrates the estimated grid passage probability and the dashed black lines represent the confidence intervals for the estimated curves. The broken grey lines show the population structure for the shrimp collected with the short grid (a) and the long grid (b).

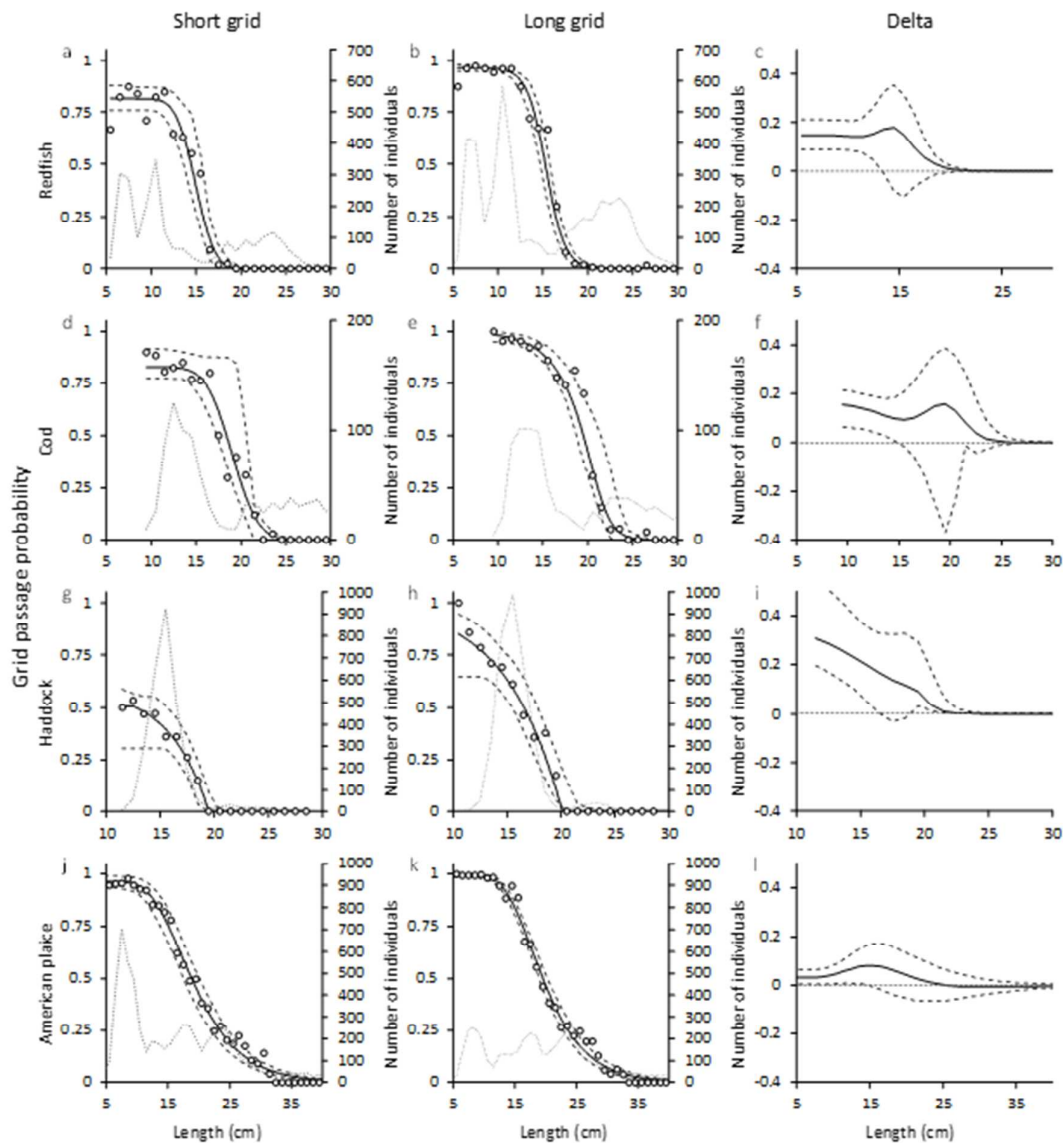


Figure 5: Size distribution and grid passage probability for redfish (a–c), cod (d–f), haddock (g–i) and American plaice (j–l) with the short grid (left column), long grid (middle column) and the difference (Delta) (right column) between both grids. The circles represent the experimental data collected during the cruise. The solid black line shows the estimated grid passage probability and the dashed black lines represent the confidence intervals for the estimated curves. The dotted grey lines show the population structure for the four bycatch species collected with the short grid (left column) and the long grid (middle column).

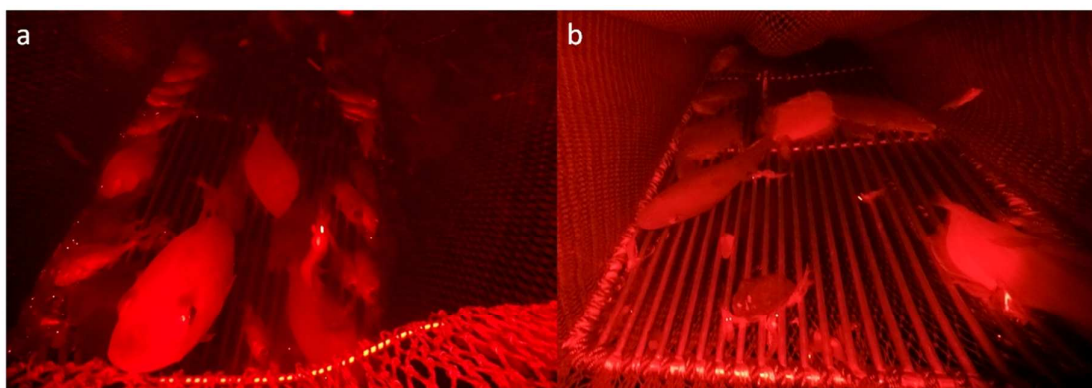


Figure 6: Stills from underwater video recordings showing blockage by fish of the short (a) and long (b) sorting grids tested during the trials. The stills were taken approximately 30 min into the haul.

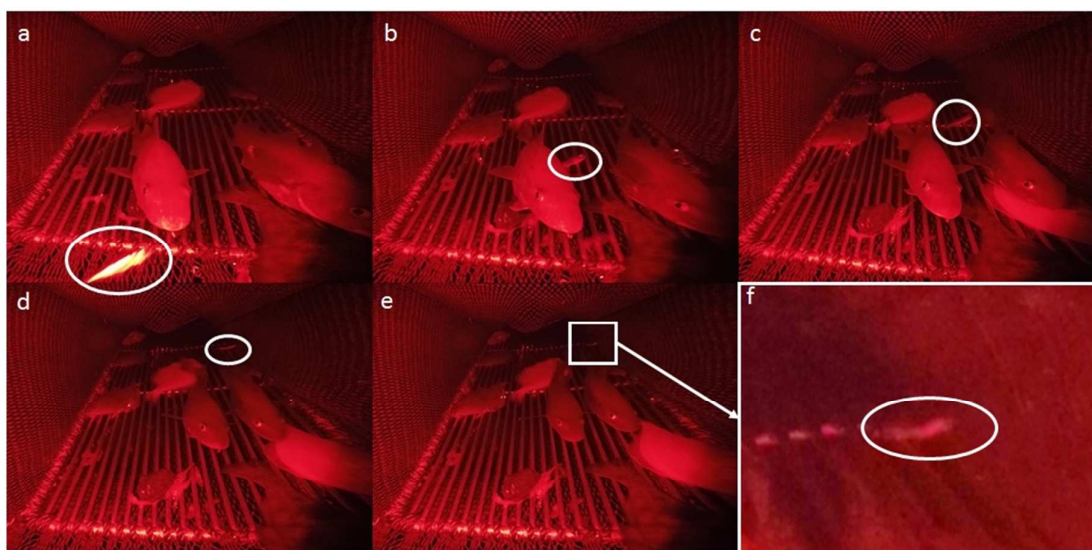


Figure 7: Images a–f showing a juvenile haddock entering the lower part of the grid area (a) and gliding along the grid (b–d), until it finally orientates itself correctly towards the grid and passes through (e–f). The sequence of images was taken from a recording made on the long grid at an angle of ca. 30°.

Table 1: Summary data of the number of individuals that were length measured from individual hauls conducted with the short and long grid, respectively. Values in parentheses are subsampling ratios shown as percentages (weight ratio for shrimp and number ratio for fish) provided only when subsampling took place. S: short grid, L: long grid. *ng*: Numbers in grid cover. *nc*: Numbers in codend.

Haul	Grid	D. shrimp		Redfish		A. plaice		Cod		Haddock	
		<i>ng</i>	<i>nc</i>	<i>ng</i>	<i>nc</i>	<i>ng</i>	<i>nc</i>	<i>ng</i>	<i>nc</i>	<i>ng</i>	<i>nc</i>
1	S	60(83.6)	162(3.1)	8	18	182	278	6	7	37	12
2	L	0	144(5.8)	187	108	67	76	3	8	22	25
3	L	4	204(6.6)	149	61	80	88	2	8	27	19
4	S	121(51.3)	195(4.7)	103	82	299	200	20	5	118	26
5	S	165(75.1)	201(2.1)	104	103	175	281	15	12	117	59
6	L	8	211(1.9)	66	155	243	176	3	5	79	100
7	L	18	220(1.3)	110	407	203	309	26	33	175	402
8	S	127(27.9)	187(1.0)	167	320	238	297	87	88	340	348
9	S	193(73.2)	222(1.4)	75	214	230	403	57	45	81	89
10	L	222(33.5)	198(1.3)	140	417	284	264	72	94	105	172
11	L	9(58.5)	239(1.5)	29	72	132	218	16	24	11	29
12	S	54(80.1)	174(2.3)	30	15	218	271(34.2)	55	9	7	7
13	S	16(82.3)	179(5.0)	80	18	91	226	16	3	25	19
14	L	10(86.2)	172(3.9)	169	33	200	264	13	6	49	56
15	L	8(83.0)	174(3.4)	215	53	141	310	15	8	44	43
16	S	96(73.5)	217(1.9)	71	31	234	423	37	3	61	23
17	S	181(23.7)	198(1.4)	186	28	387	610	85	14	191	52
18	L	13(71.6)	168(1.7)	312(63.9)	528	246	295	138	143	764	521
19	L	29(68.1)	202(1.5)	370	524	305	359	165	182	276	540
20	S	148(19.3)	237(1.1)	358	420	341	531	253	276	794	413
sum		1482	3904	2929	3607	4296	5879	1084	973	3323	2955

Table 2: Akaike's information criterion (AIC) values for the eight models tested on the data collected for shrimp and four bycatch fish species with the short and long grids. The lowest AIC values for each of the cases are shown in bold.

C_{grid}		Fixed at 100%				Estimated			
Model for $rc(l, \nu)$		Logit	Probit	Gompertz	Richard	Logit	Probit	Gompertz	Richard
Deep-water shrimp	Short	26768.78	26751.74	26738.52	26746.68	26770.78	26753.74	26740.52	26748.68
	Long	9096.03	9093.26	9091.07	9094.26	9098.03	9095.26	9093.07	9096.26
Redfish	Short	1789.01	1788.08	1913.14	1669.20	1639.14	1638.15	1646.91	1638.50
	Long	1481.04	1545.39	1858.79	1400.23	1355.75	1369.67	1370.39	1357.62
American plaice	Short	4744.43	4745.83	4812.62	4742.44	4746.43	4744.95	4727.39	4729.36
	Long	3111.33	3099.73	3085.31	3073.98	3113.33	3101.73	3067.64	3069.64
Cod	Short	674.84	672.71	712.12	647.82	647.29	645.82	650.64	647.10
	Long	419.92	423.20	460.37	411.29	412.80	414.11	421.57	412.65
haddock	Short	3551.68	3547.18	3558.43	3527.06	3532.39	3531.09	3538.18	3526.01
	Long	4314.55	4311.37	4334.31	4300.37	4303.31	4300.52	4306.26	4302.37

Table 3: Parameter values and fit statistics for selected models. Values in parentheses are 95 % confidence limits. Note that $L50_{grid}$ and SR_{grid} are provided in millimetres (carapace length) for Deep-water shrimp and in centimetres (total length) for the bycatch fish species.

	Deep-water shrimp		Redfish		American plaice		Cod		Haddock	
Grid	Short	Long	Short	Long	Short	Long	Short	Long	Short	Long
Model for $rc(l, \nu)$	Gompertz	Gompertz	Probit	Logit	Gompertz	Gompertz	Probit	Richard	Richard	Richard
C_{grid} (%)	Fixed to 100	Fixed to 100	81.7 (75.8-87.6)	96.2 (94.8-97.6)	96.1 (93.3-98.8)	99.4 (98.3-100.0)	82.8 (77.4-91.3)	Fixed to 100	59.0 (35.1-100.0)	Fixed to 100
$L50_{grid}$ (mm/cm)	57.3 (50.2-75.1)	116.6 (82.5-165.9)	14.9 (14.2-15.8)	15.4 (14.8-15.8)	19.1 (18.0-20.3)	19.6 (19.0-20.4)	19.0 (17.8-20.7)	19.5 (18.7-21.5)	17.0 (12.7-18.4)	16.6 (15.5-17.8)
SR_{grid} (mm/cm)	34.5 (27.8-49.4)	78.1 (45.4-100.0)	2.3 (0.9-3.1)	2.3 (1.7-2.8)	8.1 (7.3-8.8)	7.3 (6.6-8.1)	3.1 (0.2-4.1)	3.7 (3.0-5.6)	3.9 (0.6-11.2)	5.6 (3.8-7.3)
L/δ	-	-	-	-	-	-	-	0.35 (0.01-0.80)	0.008 (0.003-1.41)	0.008 (0.005-0.47)
p-value	<0.001	0.005	0.570	0.232	0.119	0.198	0.999	0.996	0.892	0.425
Deviance	68.83	38.34	35.83	41.84	53.01	50.63	11.48	12.67	8.72	17.44
DOF	19	19	38	36	42	43	29	29	15	17

Table 4: Catch efficiency indicator values according to equation (5). For Deepwater shrimp only individuals above 15 mm carapace length are included. For bycatch species all sizes are included. Values in parentheses represents 95% confidence limits.

	nP_{+short}	nP_{+long}	$\Delta nP_{+} = nP_{+long} - nP_{+short}$
Deep-water shrimp	97.04(95.88-98.15)	99.10(97.68-99.89)	2.06(0.36-3.62)
Redfish	51.38(34.69-60.69)	55.07(42.47-66.68)	3.69(-13.10-24.75)
American plaice	62.79(55.71-69.00)	55.38(50.70-60.10)	-7.41(-15.31-0.86)
Cod	42.27(21.45-49.64)	52.80(49.69-56.78)	10.53(2.47-31.67)
Haddock	37.18(26.54-45.86)	55.13(43.99-66.13)	17.95(3.76-33.93)

Draft

1 Appendix

2 Size selection models

3 The basic size selection models used in the present study are presented below (Wileman et
4 al., 1996).

5 The Logistic (*Logit*) size selection curve is the cumulative distribution function of a logistic
6 random variable:

$$\text{Logit}(l) = \frac{\exp(a + bl)}{1 + \exp(a + bl)}$$

7 Where a and b are the parameters of the model. *Logit*(l) quantifies the length-dependent
8 retention probability with l being the length of the fish or shrimp. The above equation can be
9 rewritten in terms of the parameters $L50$ and SR , where:

$$L50 = -a/b, \quad SR = \frac{2 \times \ln(3)}{b} = \frac{\ln(9)}{b}$$

10 Leading to:

$$\text{Logit}(l) = \left(\frac{\exp\left(\frac{\ln(9)}{SR} \times (l - L50)\right)}{1 + \exp\left(\frac{\ln(9)}{SR} \times (l - L50)\right)} \right)$$

11 The *Probit* size selection curve (Normal probability ogive) is the cumulative distribution of a
12 normal random variable,

$$\text{Probit}(l) = \Phi(a + bl)$$

Where Φ is the cumulative distribution function of a standard normal random variable, and a and b are the parameters of the model. The *Probit* can be rewritten in terms of parameters $L50$ and SR , where:

$$L50 = -a/b, \quad SR = \frac{2 \times Probit(0.75 - 0.25)}{b} \approx \frac{1.349}{b}$$

Leading to:

$$Probit(l) \approx \left(\frac{\exp\left(\frac{1.349}{SR}(l - L50)\right)}{1 + \exp\left(\frac{1.349}{SR}(l - L50)\right)} \right)$$

17

The *Gompertz* size selection curve is expressed by the following equation:

$$Gompertz(l) = \exp(-\exp(-(a + bl)))$$

It can be rewritten in terms of the parameters $L50$ and SR , where:

$$L50 = \frac{-\ln(-\ln(0.5)) - a}{b} \approx \frac{0.3665 - a}{b}, \quad SR = \frac{\ln\left(\frac{\ln(0.25)}{\ln(0.75)}\right)}{b} \approx \frac{1.573}{b}$$

Leading to:

$$Gompertz(l) \approx \exp\left(-\exp\left(-\left(0.3665 + \frac{1.573}{SR}(l - L50)\right)\right)\right)$$

The last of the four basic size selection curves considered here is the *Richard* curve, which has an extra parameter, named $1/\delta$. This parameter controls the degree of asymmetry of the curve. When $\delta = 1$ the curve is identical to the *Logit* curve. The equation for a Richard size selection curve is the following:

$$Richard(l) = \left(\frac{\exp(a + bl)}{1 + \exp(a + bl)} \right)^{1/\delta}$$

25 Rewritten in terms of the parameters $L50$ and SR with:

$$L50 = \frac{Logit(0.5^\delta) - a}{b}$$

$$SR = \frac{Logit(0.75^\delta) - Logit(0.25^\delta)}{b}$$

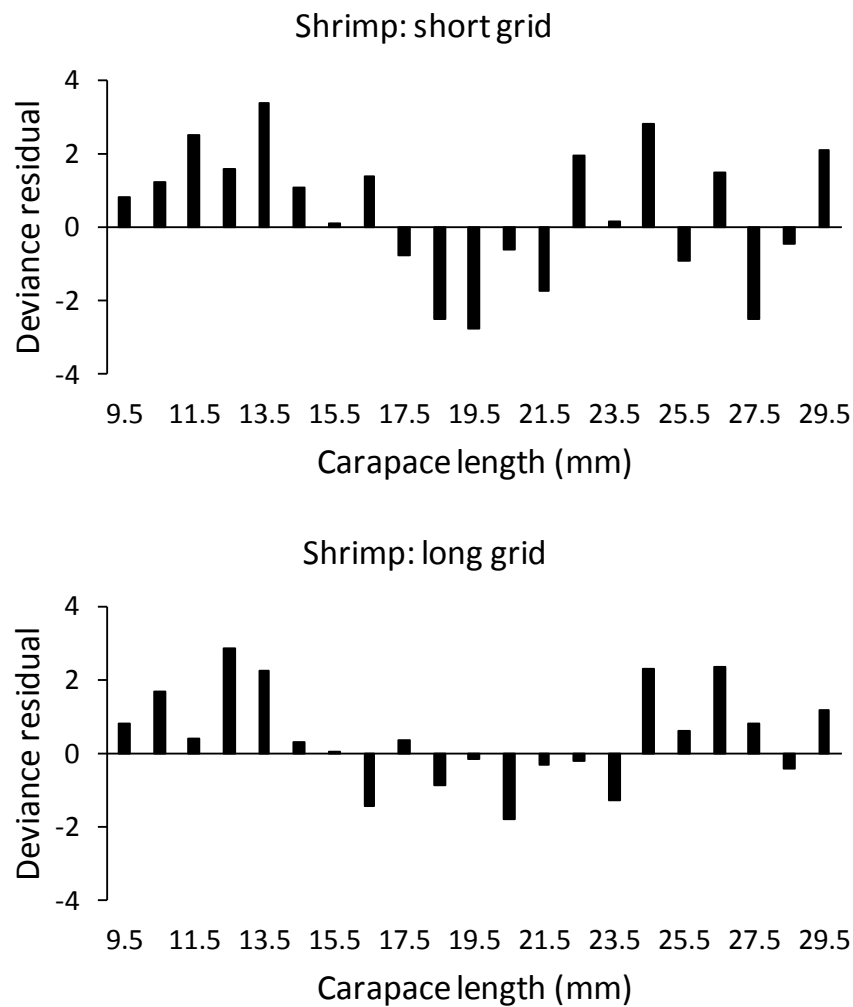
26 Leading to:

$$Richard(l) = \left(\frac{\exp \left(Logit(0.5^\delta) + \left(\frac{Logit(0.75^\delta) - Logit(0.25^\delta)}{SR} \right) (l - L50) \right)}{1 + \exp \left(Logit(0.5^\delta) + \left(\frac{Logit(0.75^\delta) - Logit(0.25^\delta)}{SR} \right) (l - L50) \right)} \right)$$

27

Deviance residual plots

Figure A1 provides (in accordance to Wileman et al. (1996)) deviance residual plots for the modelling of the length grid passage probability for shrimp, for respectively the short and long grid.



32

33 Figure A1: Deviance residual plots for modelling of length-dependent grid passage
34 probability for shrimp and for respectively short (top) and long grid (bottom).